Publication P5

Seman, S., Iov, F., Niiranen, J., Arkkio, A. 2005. “Comparison of Simulators for Variable Speed Wind Turbine Transient Analysis”, *International Journal of Energy Research*, Vol. 30, Issue 9, pp. 713-728, Available: http://www3.interscience.wiley.com/cgi-bin/fulltext/112579563/PDFSTART, 16 p., (7.5.2006).

INTERNATIONAL JOURNAL OF ENERGY RESEARCH
Int. J. Energy Res. 2006; **30**:713–728
Published online 10 April 2006 in Wiley InterScience (www.interscience.wiley.com). DOI: 10.1002/er.1183

Comparison of simulators for variable-speed wind turbine transient analysis

S. Seman[1,*,†], F. Iov[2], J. Niiranen[3] and A. Arkkio[1]

[1] *Laboratory of Electromechanics, Helsinki University of Technology, P.O. Box 3000, FIN-02015 HUT, Finland*
[2] *Institute of Energy Technology, Aalborg University. Pontoppidanstraede 101, DK-9220 Aalborg Øst, Denmark*
[3] *ABB Oy, P.O. Box 184, Helsinki, FIN-00381, Finland*

SUMMARY

This paper presents a comparison of three variable-speed wind turbine simulators used for a 2 MW wind turbine short-term transient behaviour study during a symmetrical network disturbance. The simulator with doubly fed induction generator (DFIG) analytical model, the simulator with a finite element method (FEM) DFIG model and the wind turbine simulator with an analytical model of DFIG are compared. The comparison of the simulation results shows the influence of the different modelling approaches on the short-term transient simulation accuracy. Copyright © 2005 John Wiley & Sons, Ltd.

KEY WORDS: analytical model; doubly fed induction generator; FEM; modelling; short-term transient; simulator; variable-speed wind turbine; wind power

1. INTRODUCTION

The variable-speed wind turbines with doubly fed induction generators (DFIG) are nowadays more widely used in wind-power generation mainly due to their ability to supply power at constant voltage and frequency while the rotor speed varies. Together with the increase of the number of the DFIG wind turbines connected to the network, the new network codes were issued prescribing how the wind generator has to support the network during the power disturbances in the network, for example, E.ON. (2003), Eltra (2004). Therefore, it is necessary to carry out accurate transient simulations in order to understand the impact of the power system disturbances on a wind turbine operation.

The DFIG wind turbine models that are used in transient analyses presented by Ekanayake *et al.* (2003), Slootweg *et al.* (2001), Holdsworth *et al.* (2003), Tapia *et al.* (2003) represent the generator by means of a two-axis-theory-based model with constant lumped parameters. The model of DFIG that takes into account the equivalent circuit parameter variation was presented by Seman *et al.* (2004a).

*Correspondence to: S. Seman, Laboratory of Electromechanics, Helsinki University of Technology, P.O. Box 3000, FIN-02015 HUT, Finland.
†E-mail: slavomir.seman@hut.fi

Received 19 June 2005
Revised 29 September 2005
Accepted 18 October 2005

The model of the wind turbine is usually represented by a simplified model in which the wind speed and pitch angle are considered to be constant and the reference value of electromagnetic torque is obtained from optimum torque–speed curve as it was done, for example, by Arnalte *et al.* (2002) or, for instance, by aerodynamic filter approach presented by Petru and Thiringer (2002). A rather detailed model of the variable-speed wind turbine has been presented by Akhmatov (2002).

A significant part of the wind turbine model is the model of a frequency converter that supplies the rotor of the DFIG. As it was stated by Akhmatov (2002), the converter is found to be the most sensitive part of the wind turbine when subjected to a short-circuit fault in the grid. Frequency converter models are, in most cases, represented by two back-to-back connected voltage source inverters, one being on the network side and the other on the rotor side.

The control of a frequency converter is usually based on field-oriented control as shown by Pena *et al.* (1996) and also the modified DTC could be used as presented by Gokhale *et al.* (2004). The frequency converters are usually equipped with a rotor over-current protection circuit that is commonly called crowbar, which was described by Niiranen (2004) and Seman *et al.* (2004a,b). The crowbar protects the rotor-side frequency converter while DFIG generates high grid current during the disturbance.

The simulators presented in this paper are used for a 2 MW wind turbine network disturbance transient behaviour study. The mechanical part of the wind turbine model consists of the rotor aerodynamic model, wind turbine control and the drive train model. The DFIG is represented by an analytical two-axis model with constant lumped parameters and by a finite element method (FEM)-based model. The model of the DFIG is coupled with the model of the passive crowbar protected and DTC-controlled frequency converter, the model of the main transformer and a simple model of the grid. The simulation results obtained by means of the detailed wind turbine simulator are compared with results obtained from a simplified simulator with an analytical model and FEM model of DFIG. The comparison of the results shows the influence of the different modelling approaches on the short-term transient simulation accuracy.

2. DESCRIPTION OF THE SIMULATORS

Three kinds of DFIG wind turbine dynamic simulators were developed and benchmarked in order to investigate the influence of the different modelling approaches on the accuracy of a short-term transient analysis.

2.1. Simulator with an analytical DFIG model

The analytical two-axis model of the DFIG with constant lumped parameters is coupled with the model of the DTC-controlled frequency converter protected by a passive crowbar, the model of the main transformer and a simple model of the grid. The mechanical part of wind turbine model and its control are omitted. The mechanical speed is considered to be constant as well as wind turbine reference torque. The simulator has been experimentally validated by full-power laboratory test (Seman *et al.*, 2005).

2.2. Simulator with FEM model of DFIG

The FEM model of the DFIG is coupled by means of an indirect procedure Kanerva *et al.* (2003) with the circuit model of the DTC-controlled frequency converter equipped with passive crowbar, the circuit model of the main transformer and a simple model of the grid. The model of the wind turbine mechanical part and its control are omitted. Similarly as in previous simulator, the mechanical speed is considered to be constant as well as wind turbine reference torque. The simulator has been experimentally validated by full-power laboratory test (Seman *et al.*, 2005).

2.3. Wind turbine simulator with DFIG analytical model

The DFIG is represented by an analytical two-axis model with constant lumped parameters and similarly as in case of simplified model is coupled with the model of the DTC-controlled frequency converter with passive crowbar, the model of the main transformer and a simple model of the grid. The mechanical part of wind turbine model consists of the rotor aerodynamic model, the wind turbine control and the drive train model. The mechanical speed of the wind turbine is calculated from the drive train model and the wind turbine control determinates the reference torque.

3. MODELLING OF THE WIND TURBINE MECHANICAL PART AND ITS CONTROL

3.1. Turbine model

The aerodynamic model of the wind turbine rotor is based on the power coefficient C_P look-up table as it is presented by Iov *et al.* (2004). The aerodynamic torque can be determined using the power coefficient C_P based on

$$T_{\mathrm{wt}} = 0.5\pi\rho R^2 v_\infty^3 C_P \tag{1}$$

where ρ is the air density, R is the blade radius, v_∞ is the wind speed and C_P is the power coefficient.

It is important to underline that C_P coefficient for variable pitch/speed wind turbines is a function of the tip speed ratio λ and pitch angle θ as shown in Figure 1.

For reasons of clarity the power coefficient is plotted in Figure 1 for few values of the pitch angle while the look-up table used in the model contains the power coefficient for values of the pitch angle from -90° to $+90^\circ$ and tip speed ratio in the range 0–20.

The tip speed ratio is defined as

$$\lambda = \frac{\Omega R}{V_\infty} \tag{2}$$

where Ω is the rotational speed of the wind turbine.

3.2. Drive train model

The model of a wind turbine drive train is basically a three-mass model with flexible shafts both on wind turbine and generator sides. The masses correspond to a large mass of the wind turbine rotor, a mass for the gearbox wheels and a mass for generator, respectively. The moments of

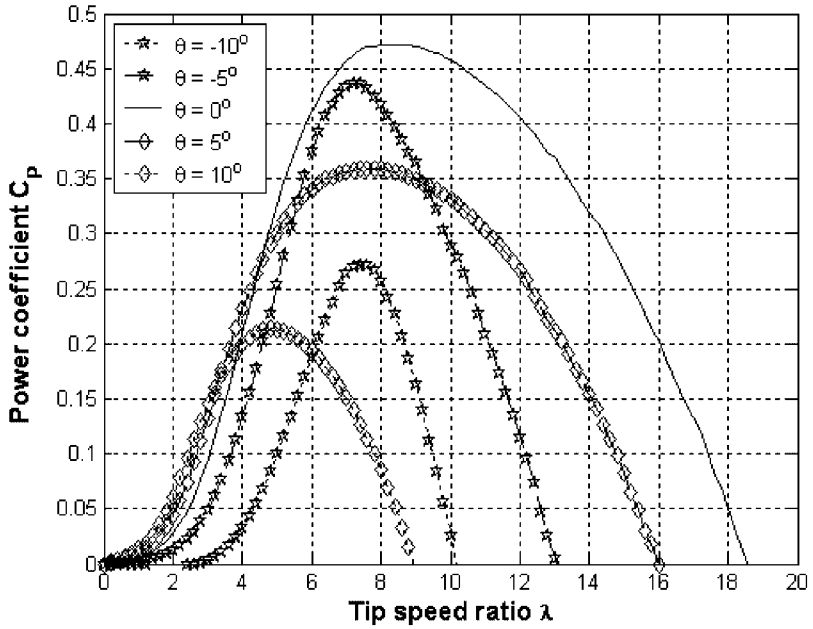

Figure 1. Power coefficient curves for a modern three blades wind turbine.

inertia for the shafts and gearbox wheels can be neglected because they are small compared with the moment of inertia of the wind turbine or generator. Thus, this model can be reduced as shown by Hansen *et al.* (2003) to a two-mass model by considering an equivalent system with an equivalent stiffness and damping factor on the wind turbine rotor side as depicted in Figure 2. The dynamic equations of the drive train are expressed as in Hansen *et al.* (2004).

3.3. Wind turbine control

The control system of a variable-speed wind turbine with DFIG has as the main goals to control the reactive power interchanged between the generator and grid and to track the wind turbine optimum operation point or to limit the output power in the case of high wind speeds (Hansen *et al.*, 2003, 2004). The overall control system of a variable-speed DFIG wind turbine is shown in Figure 3.

Two levels of control with different bandwidths and strongly connected to each other can be observed in this control scheme, namely the wind turbine control and the generator control.

The wind turbine control has slow dynamics compared with the generator control and contains two cross-coupled controllers: a speed controller and a power limitation controller. This control level supervises both the pitch angle actuator system of the turbine and the torque set point of the generator control level.

The control method used in this study is based on the two static optimum curves: mechanical power of the wind turbine versus wind speed and electrical power versus generator speed as shown in Figure 4.

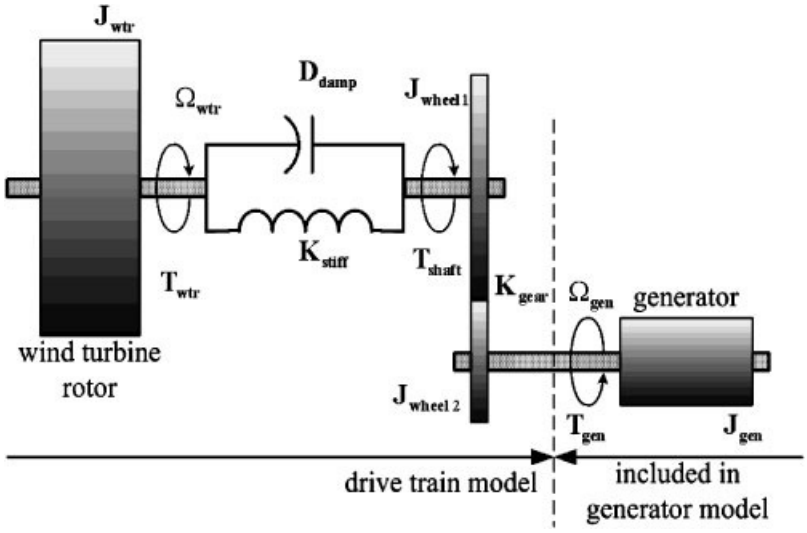

Figure 2. Equivalent model of a wind turbine drive train.

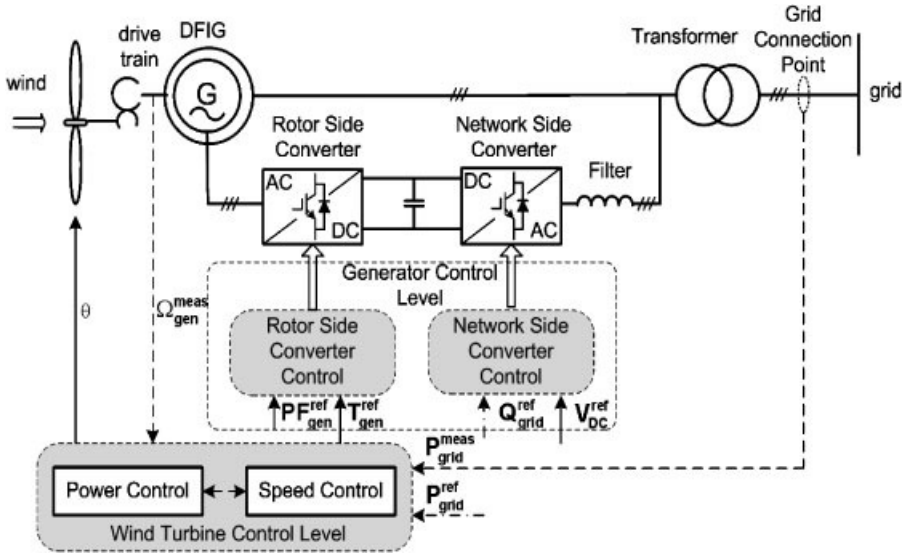

Figure 3. Overall control system of a variable-speed wind turbine with DFIG.

These characteristics are determined based on predefined aerodynamic data of the wind turbine. Since each wind turbine has some operational restrictions due to the mechanical loads, acceptable noise emissions, and the size and efficiency of the power converter, it is necessary to limit the stationary rotational speed to a range given by a minimum value and a rated value. However, the rated speed can be exceeded during the transients of the generator as shown in Figure 4.

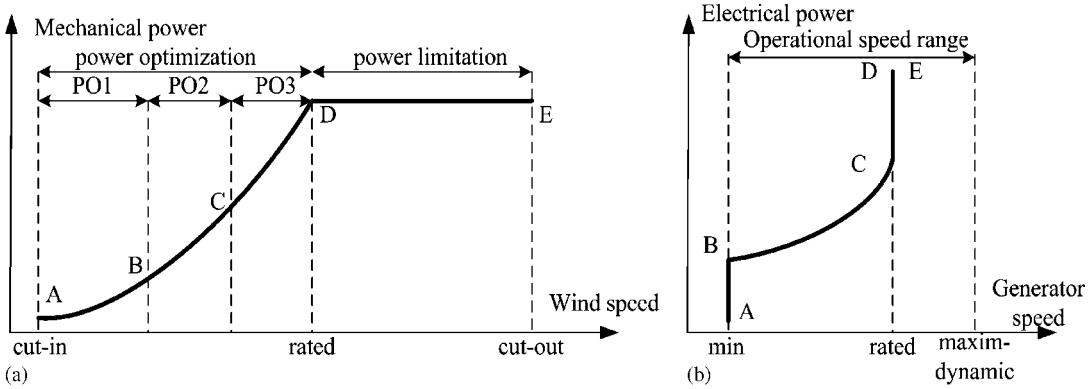

Figure 4. (a) Mechanical power versus wind speed and the operation modes for the wind turbine control; and (b) electrical power versus generator speed characteristic used in control design.

Two main control strategies for a variable-speed operation can be defined (Hansen *et al.*, 2003, 2004; Iov *et al.*, 2003):

- Power optimization strategy—from cut-in wind speed up to rated wind speed—where the energy capture is optimized mainly by changing the generator speed.
- Power limitation strategy—for wind speeds greater than the rated wind speed—where the main objective is to limit the power output of the wind turbine to its rated value.

Three operation modes can also be defined within the power optimization strategy (Hansen *et al.*, 2003; Iov *et al.*, 2003):

- PO1—partial load operation with fixed reference speed for generator speed at the lower limit.
- PO2—partial load operation with variable reference speed where the rotational speed is within minimum and the rated value.
- PO3—partial load operation with fixed reference speed at the rated value.

In power limitation, the wind turbine operates at wind speeds higher than the rated value and the output power must be limited at its rated value by modifying the pitch angle. Thus, the rotational speed is kept at its rated value and the tip speed is calculated for different wind speeds. Then, the power coefficient is calculated based on

$$C_P = \frac{2P_{\text{mec}}^{\text{rated}}\lambda(v_\infty)}{\rho\pi R^5\Omega_{\text{rated}}^3} \tag{3}$$

Once the power coefficient as well as the tip speed ratio are known, the static pitch angle can then be determined from the power coefficient look-up table. Using the above-presented algorithm the control characteristics for a 2 MW wind turbine are obtained (Iov *et al.*, 2003).

Then, these characteristics are used to design the controllers from the wind turbine control level namely the speed controller and the pitch controller. Since the optimum pitch angle is zero in the power optimization mode, the pitch controller is not active. Therefore, the main

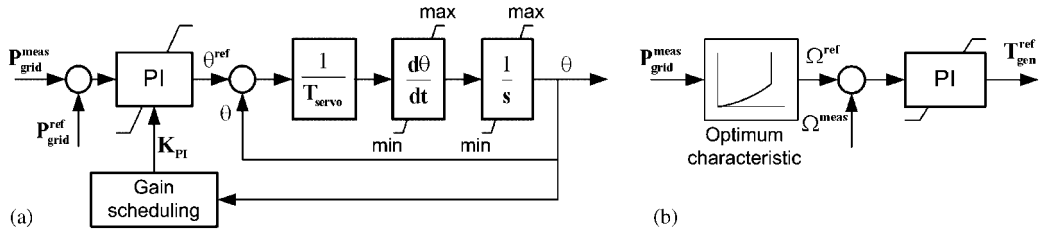

Figure 5. (a) Structure of the pitch controller for a DFIG wind turbine; and (b) structure of the speed controller for a DFIG wind turbine.

controller for this control strategy is the speed controller. In power limitation mode, both controllers are active and cross-coupled to each other.

3.3.1. Speed controller. The main tasks for the speed controller are:

- to keep the generator speed at its lower limit for PO1 strategy;
- to adapt the generator speed, and therefore to maintain the optimum tip speed ratio for PO2 strategy; and
- to keep the generator speed at its rated value and to allow dynamic variations in a predefined range in PO3 and power limitation strategy.

The structure of this controller is presented in Figure 5. Based on the measured power in the connection point of the wind turbine and using the optimum characteristic of the generator speed, the reference torque for the generator control level is obtained.

3.3.2. Pitch controller. In order to limit the output of the wind turbine at its rated value, the pitch controller has the main task to modify the pitch angle. The structure of this controller is shown in Figure 5.

The error signal between the measured power in the connection point and reference power is applied in a PI controller, which produces the reference pitch angle. This reference is compared with the actual pitch angle and the pitching servomechanism corrects the error between these two signals. The model accounts for the time constant of the servomechanism and the limitation of both pitch angle and its gradient so that a realistic response of the control system is obtained.

Since for high wind speeds there is a nonlinear relation of the pitch angle with the wind speed, a nonlinear control (gain scheduling) is used. Instabilities at high-wind speeds would be obtained if a linear control were used. More details of the gain scheduling and its impact on the stability of the control loop are presented by Hansen *et al.* (2004).

4. MODELLING OF DFIG

4.1. Equivalent circuit-based analytical model of DFIG

The generator is represented by 'T' equivalent circuit-based model with constant lumped parameters. The machine equations are written in an x–y reference frame fixed with rotor. The detailed description of DFIG dynamic model is presented by Seman *et al.* (2004b).

Table I. Parameters of the DFIG.

P_N	Rated power	1.7 MW
$U_{N,s}$	Rated stator voltage	690 V (delta)
$U_{\max,r}$	Maximum rotor voltage	2472 (star)
f_N	Rated stator frequency	50 Hz
n_N	Nominal speed	1500 rpm

4.2. Finite element model of DFIG

The magnetic field in the generator is modelled by two-dimensional finite element analysis and coupled with the voltage equations of the windings (Arkkio, 1987). The FEM computation is implemented as a functional block in Matlab-Simulink using dynamically linked program code (S-function). The voltages of the phase windings in stator and rotor are given as input variables and the phase currents, electromagnetic torque, rotational speed, rotor position and flux linkages in stator and rotor are obtained as output variables.

In time-stepping simulation, the FEM computation is coupled with Matlab-Simulink by an indirect procedure Kanerva *et al.* (2003). The finite element mesh of the DFIG covers one quarter of the cross-section, comprising 949 nodes and 1848 linear triangular elements. The parameters of the DFIG are presented in Table I.

5. MODELLING OF FREQUENCY CONVERTER AND NETWORK

5.1. Network-side converter model

The network-side converter is represented in simulation by a transfer function of the first-order discrete filter. The aim of the control of the network-side converter is to supply the dc-link and to maintain the level of dc-link voltage U_{dc} on a pre-set value. The dc-link voltage is controlled by PI-controller-based algorithm.

5.2. Rotor-side converter model

The rotor-side converter is supplied from a common dc-link and the switches are assumed to be ideal. The rotor-side frequency converter is controlled by modified DTC strategy (Gokhale *et al.*, 2004). The block structure of the rotor side DTC converter is described in detail by Seman *et al.* (2004a,b).

The reference values of the electromagnetic torque T_{e_ref} as well as rotational speed ω_{r} are considered to be constant in a case of simplified model. In the case of the detailed model when the wind turbine control is also considered, the reference torque T_{e_ref} is determined by the speed controller described in Section 3. The modulus of the desired rotor flux command obtained from the reference flux calculator as function of the power factor $PF_{\_\mathrm{ref}}$, T_{e_ref} and grid flux.

The torque and flux hysteresis comparators provide logical output that is used together with rotor flux estimate for switching pattern establishment defined by switching table. When the switching pattern is established, a voltage vector is applied to the rotor and this voltage will

change the rotor flux. The tangential component of the voltage vector controls the torque whereas the radial component increases or decreases the flux magnitude.

5.3. Crowbar

The passive crowbar is connected between the rotor of DFIG and rotor side (Niiranen, 2004; Seman *et al.*, 2004b). The crowbar eliminates high rotor currents during power systems disturbances when the stator of the generator cannot be disconnected from the network and the generator supports the network.

The main crowbar thyristor is turned on when the dc-link voltage reaches its maximum value. Simultaneously, the IGBTs of the rotor-side frequency converter are turned off. The rotor remains connected to the crowbar until the main circuit breaker disconnects the stator from the network and the rotor currents decay to zero.

5.4. Model of the network

A simple model represents the network with a three-phase voltage source in series with a short-circuit inductance and resistance.

The transmission line between the network and the transformer is modelled with its resistance, inductance and capacitance by π-equivalent circuit.

The transformer model contains a short-circuit resistance and inductance and stray capacitance of the winding. The transformer is considered to be linear, i.e. magnetic saturation has not been taken into account.

6. SIMULATION RESULTS AND DISCUSSION

The simulation analysis was carried out in Matlab-Simulink simulation environment. The system simulator was running with the time step $\Delta t = 50\,\text{ns}$ and Forward Euler method has been used. The simulation results are presented in per-unit system with the base values corresponding to the amplitudes of the respective quantities $V_{\text{base}} = 563\,\text{V}$, $I_{\text{base}} = 2.03\,\text{kA}$, $T_{\text{base}} = 10.9\,\text{kNm}$. The turn's ratio from rotor to stator is $t_{\text{r}} = 3.6$.

6.1. Synchronization of DFIG and steady state operation

In the first sequence of simulation the DFIG is synchronized with the network and after 2.5 s the rotor-side converter starts to control DFIG in torque control mode.

After synchronization the mechanical speed in simulator with DFIG analytical model is set to constant value $\omega_{\text{r}} = 1.173$ p.u. and reference torque is set to constant value $T_{\text{ref}} = -0.89$ p.u.

In a case of the wind turbine simulator with DFIG analytical model the speed controller determines the reference torque after the synchronization. The demanded value of the active power was set to $P_{\text{ref}} = 1.04$ p.u. in order to get the value of the reference torque to about $T_{\text{ref}} = -0.89$ p.u. The mechanical speed of the generator slightly oscillates around a value $\omega_{\text{r}} = 1.12$ p.u. during operation in the power limitation mode. The speed of wind was considered constant $v_{\infty} = 11\,\text{m s}^{-1}$. The reference value of power factor was set to 1.

Figure 6 shows the variation of the speed, grid active power and generator active and reactive power in steady state operation. The generator active power reaches the steady state value that

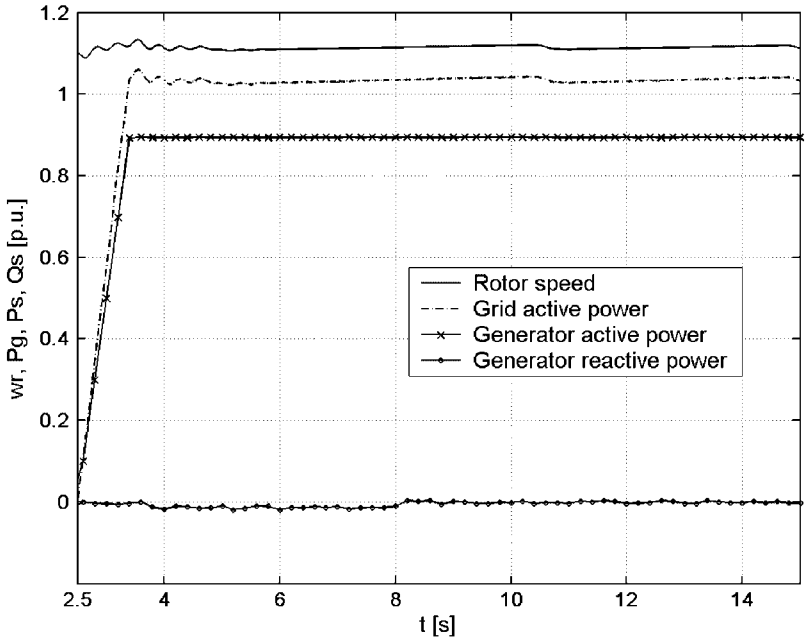

Figure 6. Rotor speed (solid), grid active power (dash–dot) and generator active(solid 'x') and reactive power (solid 'o') in steady state operation.

corresponds to the value of the reference torque and generator reactive power slightly oscillates around the zero value. The pitch controller in power limiting mode controls the grid power according to the demanded value that is set to the pitch controller.

6.2. Transient behaviour of DFIG during a grid disturbance

The network disturbance is introduced at time 15.004 s, when the stator voltage decreases down to about 35% of the nominal value. At the time instance 15.12 s, the generator is disconnected from the network by opening the main circuit breaker and the frequency converter is shut down. The fault is cleared at the time instant 15.3 s.

The symmetrical grid fault causes the amplitude of the stator voltage to drop down to 35% of the nominal value in all three phases. The high transient currents in the stator and rotor cause an increase of the dc-link voltage to the trip level and the control disconnects the rotor from the frequency converter and connects the crowbar to the rotor circuit. After disconnection from frequency converter and connection to the passive crowbar, the dc-link voltage decreases slowly and reaches the nominal value.

The stator transient currents obtained from the simulator with DFIG analytical model that neglects the drive train model as well as wind turbine model and its control are compared with wind turbine simulator with DFIG analytical model in Figure 7(a). The comparison shows that there is hardly any difference at the beginning of the transient. A small difference in amplitude, which is about 0.2 p.u. can be observed between 15.07 and 15.12 s.

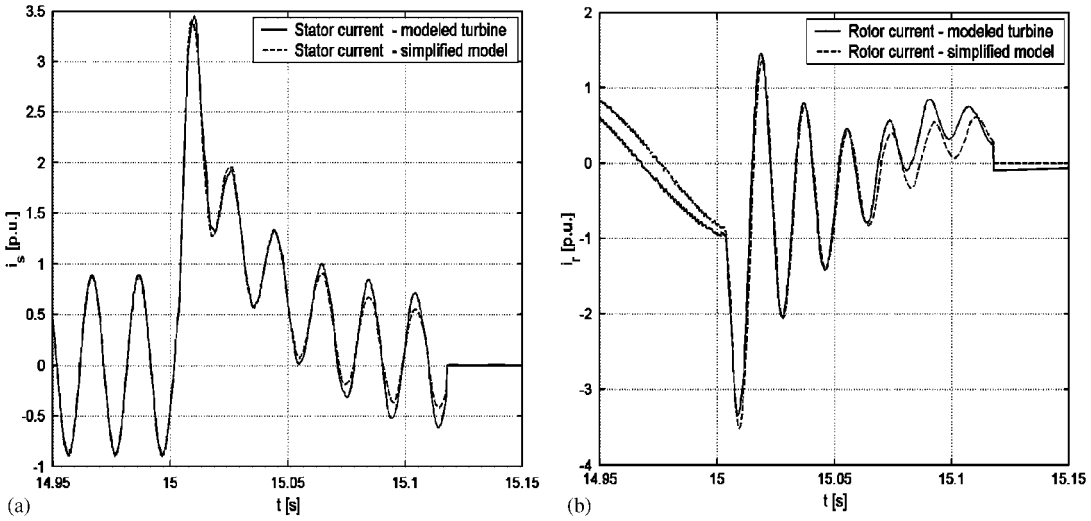

Figure 7. (a) The stator current obtained from the detailed turbine model (solid) and from simplified model (dashed) during a grid disturbance; and (b) the rotor current obtained from the detailed turbine model (solid) and from simplified model (dashed) during a grid disturbance.

The comparison of the transient rotor currents is depicted in Figure 7(b). The frequency of the rotor current calculated by the wind turbine simulator with DFIG analytical model varies due to variation of the rotor speed. The difference in frequency is well visible before the transient. In the beginning and at the end of the transient, some difference in amplitudes of the compared rotor currents can be observed. This is caused mainly by the variation of the rotor speed.

Figure 8 shows the variation of the rotor speed and also compares the generator active and reactive power during the transient. The little difference between the results can be observed at the end of the transient.

6.3. Comparison of the simulation results obtained by the simulator with DFIG analytical model and the simulator with FEM model of DFIG

The control part, frequency converter, network, transformer and crowbar were modelled in Matlab-Simulink whereas DFIG was modelled by FEM. The simulator in Simulink was running with a time step $\Delta t = 50$ ns and Forward Euler method has been used. The FEM model of DFIG was running with a time step $\Delta t_{\mathrm{FEM}} = 50\,\mu$s. The network disturbance was introduced at time 5.0037 s, when the stator voltage decreases down to about 35% of the nominal value in all three phases. At the time instant 5.12 s, the generator is disconnected from the network by opening the main circuit breaker and frequency converter is shut down. The fault is cleared at the time instant of 5.3 s.

The comparison of the simulation results obtained from the wind turbine simulator with DFIG analytical model and from the simulator with DFIG analytical model presented in the previous section shows that the complex modelling of the wind turbine and shaft system has no

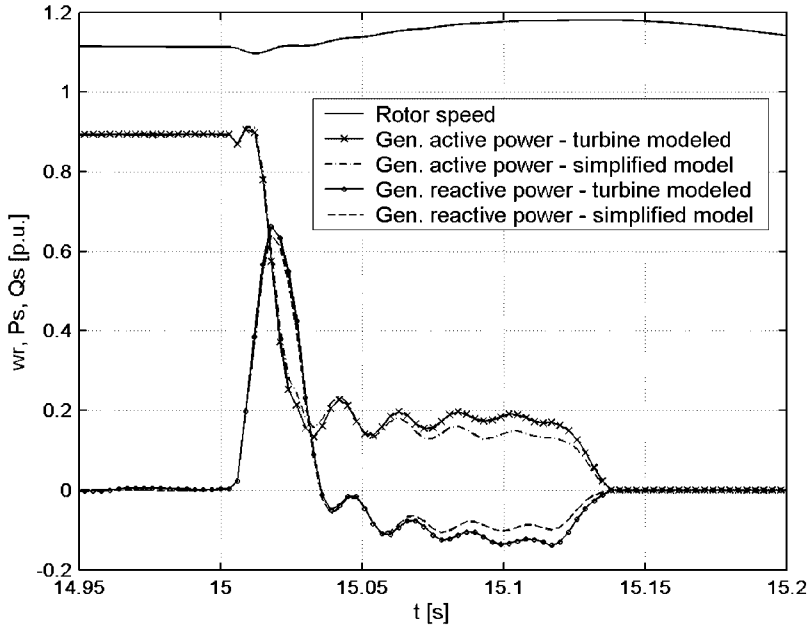

Figure 8. The rotor speed (solid), active power from the detailed model (solid 'x') and the simplified model (dash–dot), reactive power from the detailed model (solid 'o') and from the simplified model (dashed) during grid disturbance.

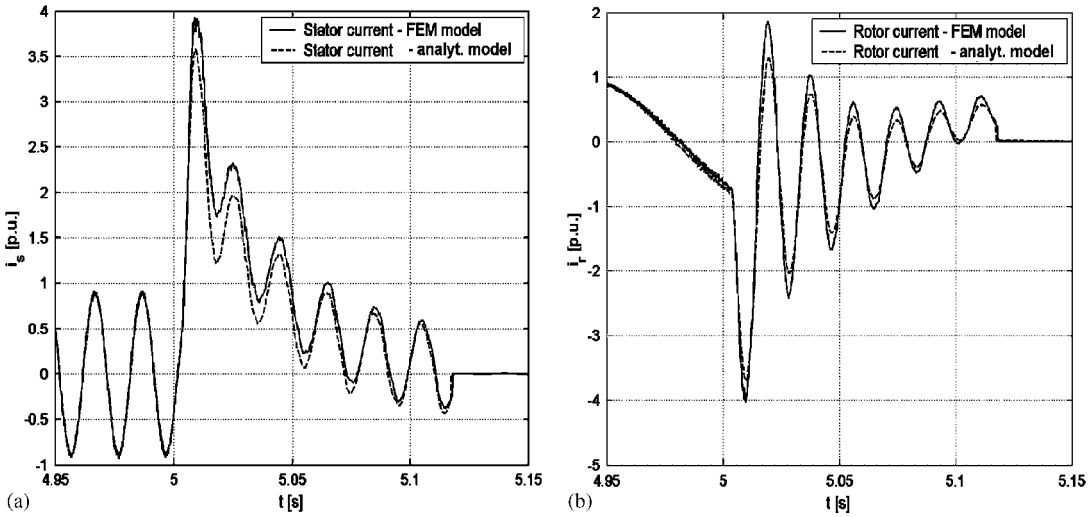

Figure 9. (a) The stator current obtained from FEM model of DFIG (solid) and from analytical model of DFIG (dashed) during a grid disturbance; and (b) the rotor current obtained from FEM model of DFIG (solid) and from analytical model of DFIG (dashed) during a grid disturbance.

significant effect on the short-term transient analysis accuracy. Therefore, the simulator with FEM model of the generator was simplified so that the models of the wind turbine and drive train were omitted. The rotor speed was set to constant value $\omega_r = 1.173$ p.u. and the reference torque to $T_{ref} = -0.89$ p.u.

The stator transient currents obtained from the analytical and FEM model of DFIG are depicted in Figure 9(a). The comparison of the simulated transient stator currents shows that the FEM current is higher and the difference is about 0.4 p.u. in the beginning of the transient. The difference is decreasing and after 5.08 s both the waveforms show good agreement.

The transient rotor current comparison is depicted in Figure 9(b). The amplitude of the rotor current calculated by FEM is, in the first period, higher than the transient rotor current calculated by the analytical model and the difference is about 0.6 p.u. The difference in amplitude is decreasing slowly and beyond the time instant of 5.1 s both curves are almost the same.

The difference in the amplitude of the transient stator and rotor current during the first period could be explained so that FEM model takes into account the magnetic saturation of the stator and rotor leakage inductances as well as the possible current displacement due to skin effect.

Figure 10 compares the generator's active and reactive power calculated by FEM model and by the simplified model. The little difference between the reactive power curves can be observed in the beginning of the transient. The active power curves are almost identical.

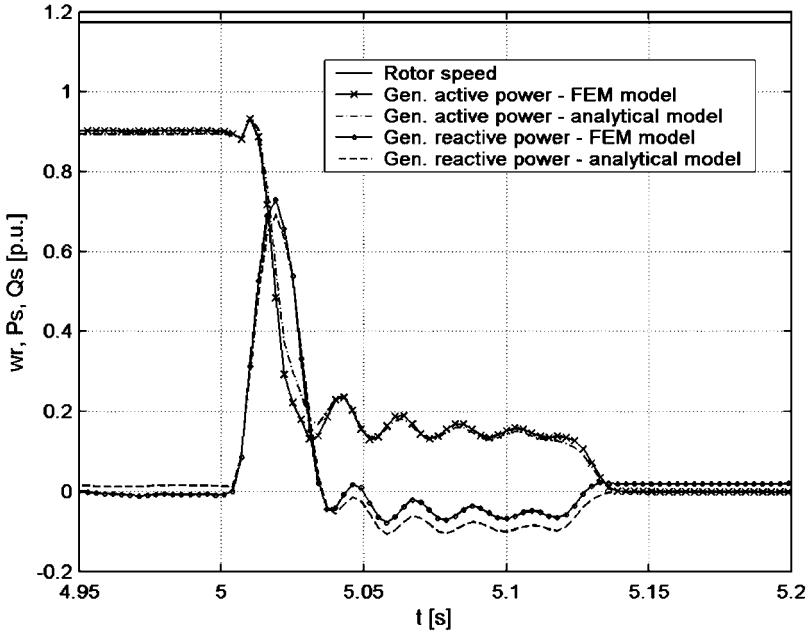

Figure 10. The rotor speed (solid), the active power from the FEM model of DFIG (solid 'x') and from the analytical model of DFIG (dash–dot), reactive power from the FEM model of DFIG (solid 'o') and from the analytical model of DFIG (dashed) during a grid disturbance.

7. CONCLUSIONS

The three simulators that were used for the 2 MW wind turbine transient behaviour study during the network symmetrical fault were presented and compared. The simulation results obtained by means of the wind turbine simulator with a DFIG analytical model were compared with results obtained from a simplified simulator with an analytical model and FEM model of DFIG. The comparison of the simulation results shows that the detailed modelling of the wind turbine and shaft system has no significant effect on the short-term transient analysis accuracy. The accuracy of a short-term transient analysis could be improved by using of the simulator with FEM model of the induction generator in which the magnetic saturation of the leakage inductances and possible current displacement due to the skin effect are taken into account. However, the comparison of the generator active and reactive power curves obtained from the different models shows that they are almost identical. Therefore, it is enough to use a simple analytical model for the transient stability and power quality study, which is not so time consuming as a FEM model.

NOMENCLATURE

C_P = power coefficient
D_{amp} = equivalent damping factor
f_N = rated stator frequency
I_{base} = base current
J_{gen} = induction generator moment of inertia
$J_{\text{wheel1,2}}$ = gearbox wheel moment of inertia
J_{wtr} = wind turbine moment of inertia
K_{gear} = gearbox ratio
K_{PI} = proportional gain
K_{stiff} = equivalent stiffness factor
n_N = generator nominal speed
$\text{PF}_{\text{\_ref}}$ = reference power factor
P_{grid} = grid active power
P_{mec} = mechanical power
P_N = rated power of induction generator
Q_{grid} = grid reactive power
R = blade radius
T_{base} = base torque
T_{e_ref} = reference electromagnetic torque
T_{gen} = induction generator torque
T_{shaft} = shaft system mechanical torque
T_{wt} = aerodynamic torque
U_{dc} = dc-link voltage
$U_{\text{max},r}$ = generator maximum rotor voltage
$U_{N,s}$ = generator rated stator voltage
v_∞ = wind speed
V_{base} = base voltage

Δt = simulation time step
Δt_{FEM} = FEM simulation time step
θ = pitch angle
λ = tip speed ratio
ρ = air density
ω_{r}, Ω_{gen} = induction generator mechanical speed
Ω = rotational speed of the wind turbine

Superscripts

meas = measured
ref = reference

REFERENCES

Akhmatov V. 2002. Modelling of variable-speed wind turbines with doubly-fed induction generators in short term stability investigations. *International Workshop on Transmission Networks for Offshore Wind Farms*, Stockholm, Sweden.

Arkkio A. 1987. Analysis of induction motors based on the numerical solution of the magnetic field and circuit equations. *Doctoral Thesis*, Acta Polytechnica Scandinavica Electrical Engineering Series, No. 59, Helsinki, Finland: http://lib.hut.fi/Diss/198X/isbn951226076X/

Arnalte S, Burgos JC, Rodrigues-Amenedo JL. 2002. Direct torque control of a doubly-fed induction generator for variable speed wind turbines. *Electric Power Components and Systems* **30**:199–216.

E.ON. 2003. Netzanschlussregeln Hoch-und Höchstspannung.

Ekanayake JB, Holdsworth L, Wu XG, Jenkins N. 2003. Dynamic modeling of doubly fed induction generator wind turbines. *IEEE Transaction on Power Systems* **18**(2):803–809.

Eltra. 2004. Specifications for connecting wind farms to the transmission network. ELT 1999-411a, www.eltra.dk

Gokhale KP, Krakker DW, Heikkilä SJ. 2004. Controller for a wound rotor slip ring induction machine. U.S. Patent 6741059. http://patft.uspto.gov

Hansen AD, Jauch C, Sørensen P, Iov F, Blaabjerg F. 2003. Dynamic wind turbine models in power system simulation tool. *Risø-R-1400*. Pitney Bowses Management Services Denmark A/S: Denmark. ISBN 87-550-3198-6.

Hansen AD, Sørensen P, Iov F, Blaabjerg F. 2004. Control of variable pitch/variable speed wind turbine with doubly fed induction generator. *Journal of Wind Engineering* **28**(4):411–432.

Holdsworth L, Wu XG, Ekanayake JB, Jenkins N. 2003. Comparison of fixed speed and doubly-fed induction wind turbines during power system disturbances. *IEE Proceedings—Generation, Transmission and Distribution* **150**(3):343–352.

Iov F, Blaabjerg F, Hansen AD. 2003. Analysis of a variable-speed wind energy conversion scheme with doubly-fed induction generator. *International Journal in Electronics* **90**(11–12):779–794.

Iov F, Hansen AD, Sørensen P, Blaabjerg F. 2004. *Wind Turbine Blockset in Matlab/Simulink General Overview and Description of the Models*. UNI.PRINT: Aalborg University, Denmark. ISBN 87-89179-46-3.

Kanerva S, Seman S, Arkkio A. 2003. Simulation of electric drive systems with coupled finite element analysis and system simulator. *10th European Conference on Power Electronics and Applications*, Toulouse, France.

Niiranen J. 2004. Voltage dip ride through of doubly-fed generator equipped with active crowbar. *Nordic Wind Power Conference*, Chalmers University of Technology, Göteborg, Sweden.

Pena R, Clare JC, Asher GM. 1996. Doubly fed induction generator using back-to-back PWM converters and its application to variable-speed wind-energy generation. *IEE Proceedings of the Electrical Power Applications* **143**(3):231–241.

Petru T, Thiringer T. 2002. Modeling of wind turbines for power system studies. *IEEE Transaction on Power Systems* **17**(4):1132–1139.

Seman S, Kanerva S, Niiranen J, Arkkio A. 2004a. Transient analysis of wind power doubly fed induction generator using coupled field circuit model. *ICEM 2004* (CD-ROM), Cracow, Poland.

Seman S, Niiranen J, Kanerva S, Arkkio A. 2004b. Analysis of a 1.7 MVA doubly fed wind-power induction generator during power systems disturbances. *NORPIE 2004*, Trondheim, Norway, http://www.elkraft.ntnu.no/norpie/10956873/Final%20Papers/046%20-%20NORP-Seman.pdf

Seman S, Niiranen J, Kanerva S, Arkkio A, Saitz J. 2005. Performance study of doubly fed wind-power generator under network disturbances. *IEEE Transaction on Energy Conversion*, to be published.
Slootweg JG, Polinder H, Kling WL. 2001. Dynamic modeling of a wind turbine with doubly fed induction generator. *IEEE Power Engineering Society Summer Meeting* **1**:644–649.
Tapia A, Tapia G, Ostolaza JX, Saenz JR. 2003. Modeling and control of a wind turbine driven doubly fed induction generator. *IEEE Transactions on Energy Conversion* **18**(2):194–204.

